analytical chemistry

pubs.acs.org/ac

Letter

Rapid and Sensitive Detection of Antigen from SARS-CoV-2 Variants of Concern by a Multivalent Minibinder-Functionalized Nanomechanical Sensor

Dilip Kumar Agarwal,[×] Andrew C. Hunt,[×] Gajendra S. Shekhawat, Lauren Carter, Sidney Chan, Kejia Wu, Longxing Cao, David Baker, Ramon Lorenzo-Redondo, Egon A. Ozer, Lacy M. Simons, Judd F. Hultquist, Michael C. Jewett,* and Vinayak P. Dravid*

Cite This: *Anal. Chem.* 2022, 94, 8105−8109

Read Online

ACCESS | Metrics & More | Article Recommendations | Supporting Information

ABSTRACT: New platforms for the rapid and sensitive detection of severe acute respiratory syndrome coronavirus 2 (SARS-CoV-2) variants of concern are urgently needed. Here we report the development of a nanomechanical sensor based on the deflection of a microcantilever capable of detecting the SARS-CoV-2 spike (S) glycoprotein antigen using computationally designed multivalent minibinders immobilized on a microcantilever surface. The sensor exhibits rapid (<5 min) detection of the target antigens down to concentrations of 0.05 ng/mL (362 fM) and is more than an order of magnitude more sensitive than an antibody-based cantilever sensor. Validation of the sensor with clinical samples from 33 patients, including 9 patients infected with the Omicron (BA.1) variant observed detection of antigen from nasopharyngeal swabs with cycle threshold (Ct) values as high as 39, suggesting a limit of detection similar to that of the quantitative reverse transcription polymerase chain reaction (RT-qPCR). Our findings demonstrate the use of minibinders and nanomechanical sensors for the rapid and sensitive detection of SARS-CoV-2 and potentially other disease markers.

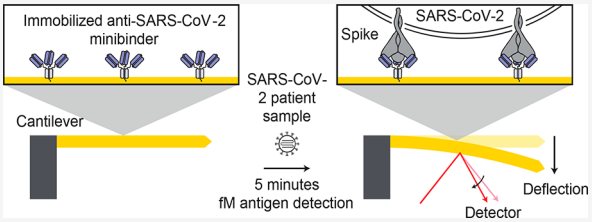

The coronavirus disease 2019 (COVID-19) pandemic caused by severe acute respiratory syndrome coronavirus 2 (SARS-CoV-2) has highlighted the importance and need for the rapid and accurate detection of pathogens for disease identification and pandemic mitigation. The gold standard techniques for the identification of viral pathogens are the detection of viral nucleic acid by quantitative reverse transcription polymerase chain reaction (RT-qPCR) or viral antigen detection through lateral flow immunoassays (LFIA).[1] RT-qPCR based techniques are highly sensitive but are relatively expensive, take hours to days to get results, and require a centralized laboratory with trained technicians.[2] LFIAs, frequently called rapid antigen tests, are cheaper, faster, useful in point-of-care settings[2] and have shown beneficial impact on population-level disease spread in widespread testing campaigns.[3,4] However, SARS-CoV-2 LFIAs have moderate to low sensitivities at viral loads below 10^7 RNA copies per mL,[5,6] which does not cover the range of viral loads where infected individuals transmit the virus,[4,5,7,8] an issue during the emergence of the B.1.1.529 (Omicron) variant of concern.[9−11] It is clear there remains a need for viral detection approaches that are rapid, sensitive, and clinically useful in point-of-care settings.

Toward addressing this need, we previously designed a nanomechanical microcantilever sensor platform that enables rapid and sensitive detection of SARS-CoV-2 N protein antigen at clinically relevant concentrations in patient samples.[12] Microcantilevers (Figure S1) are promising for disease diagnostics due to their rapid and sensitive detection of biomolecules and potential for point-of-care use.[13−15] Binding on the receptor-functionalized microcantilever results in surface stress that causes physical bending of the cantilever,[16] which can be measured optically[12] or electronically[17] (Figure 1a). Monoclonal antibodies are traditionally used for mediating specific binding of the target antigen of choice to the cantilever surface. However, they are typically nonspecifically labeled, resulting in randomly oriented proteins on the cantilever surface,[12] and they are sensitive to mutations in their target epitope and antigenic drift.[18]

As an alternative to antibodies, we recently developed multivalent minibinders, small, computationally designed binding proteins, targeting the SARS-CoV-2 S glycoprotein trimer.[19,20] The TRI2-2 multivalent minibinder, a trivalent version of the monovalent AHB2[19] minibinder, simultaneously engages all three RBDs on a single S trimer and exhibits tight binding to all tested SARS-CoV-2 variants.[20] The minibinders

Received: March 18, 2022
Accepted: May 23, 2022
Published: June 2, 2022

https://doi.org/10.1021/acs.analchem.2c01221
Anal. Chem. 2022, 94, 8105−8109

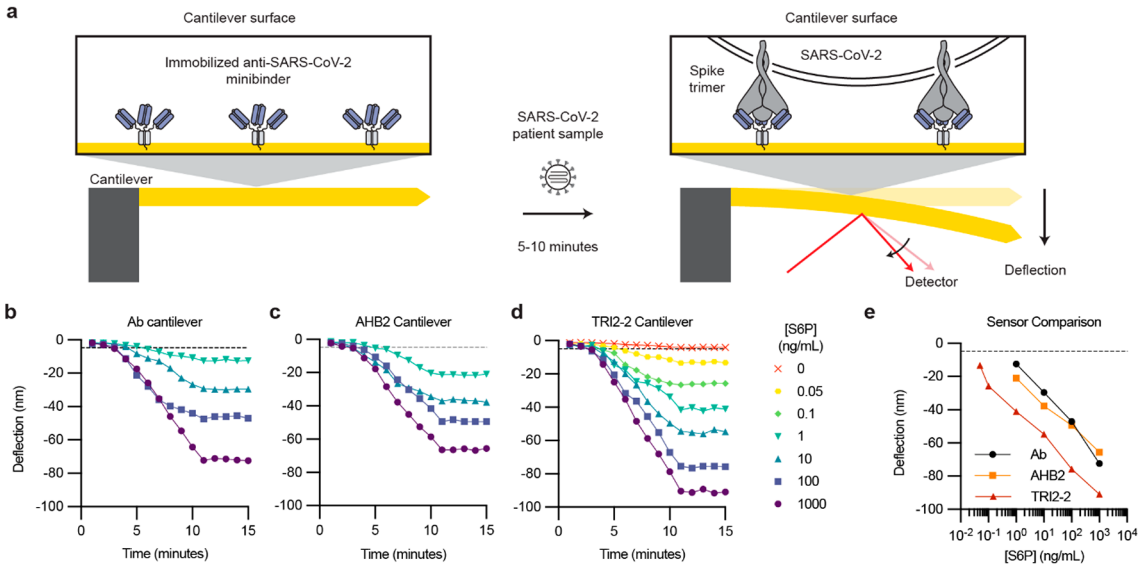

Figure 1. Cantilever-based sensing of SARS-CoV-2 spike protein (S6P). (a) Cantilever sensing mechanism; deflection is observed upon binding of the SARS-CoV-2 spike trimer to the captured binder immobilized on the cantilever. (b–d) Deflection of cantilever sensors over time with anti-S antibody (b), AHB2 (c), and TRI2-2 (d) immobilized on the cantilever (mean ± SEM, n = 3). (e) Comparison of deflection between antibody, AHB2, and TRI2-2 cantilevers after 15 min of equilibration (mean ± SEM, n = 3). For all plots, the dashed horizontal line indicates the deflection LOD cutoff (average of the combined negative control measurements ±3 standard deviations) and an absence of error bars indicates error within the marker.

are small (5–15× smaller than an antibody) and can be site specifically functionalized with a cysteine residue to enable oriented and high density immobilization on sensor surfaces.[21,22]

In this work, we evaluated the performance of microcantilever sensors functionalized with the monovalent AHB2 and trivalent TRI2-2 minibinders,[19,20] which have not been previously evaluated as sensors, for the detection of SARS-CoV-2 S antigen. We functionalized gold-coated microcantilever sensors with minibinders containing C-terminal cysteine residues, produced via cell-free protein synthesis,[23−25] and compared them to an antibody based sensor. The multivalent minibinder sensor exhibited a limit of detection (LOD) more than an order of magnitude better than that of the antibody-based sensor. Furthermore, using these sensors we observed rapid (<5 min) and sensitive detection (<0.05 ng/mL) of purified SARS-CoV-2 antigens from SARS-COV-2 variants of concern as well as detection of SARS-CoV-2 in patient nasopharyngeal swabs. S antigen is detected at a concentration corresponding to 96 genome copies per mL, indicating the sensor has an LOD on-par with RT-qPCR-based tests.[26] The developed technology is a promising diagnostic platform.

We first compared the response of cantilevers functionalized with antibody, monomeric minibinder AHB2, and trimeric minibinder TRI2-2 to detect the Wuhan-Hu-1 SARS-CoV-2 prefusion stabilized hexapro spike protein (S6P) (Figure 1).[27] Cantilever measurements were conducted in a small microfluidic chamber and deflection was monitored using an optical liquid atomic force microscopy (AFM) setup. Cantilevers were functionalized with the desired binder and then incubated with different concentrations of analytes in the sample chamber and monitored for 15 min. For all binders, the concentration of the S6P analyte exhibited a log–linear relationship with deflection, and the system reached equilibrium after approximately 10 min of incubation (Figure 1b–d). Replicates were highly concordant and exhibited low standard deviations (Figure S2, mean standard deviation = 0.64 nm). TRI2-2 cantilevers exhibited more sensitive detection than either AHB2 or the antibody-functionalized cantilevers by more than an order of magnitude (Figure 1e). At the lowest tested concentration of S6P (0.05 ng/mL or 362 fM) TRI2-2 exhibited signal significantly different from the negative control after 4 min (p = 0.032, 2-way ANOVA with Sidak's multiple comparisons test) (Figure 1d). The observed difference in response with the TRI2-2 cantilevers is likely due to the high avidity (it engages all three RBDs within an S trimer simultaneously).[20] When compared to the antibody cantilevers, the improvement may also be influenced by a greater immobilization density on the cantilever. This result indicates that TRI2-2 functionalized cantilevers are suitable sensors for the SARS-CoV-2 S trimer antigen.

We next evaluated the ability of TRI2-2 cantilevers to sense S trimer corresponding to the Alpha (B.1.1.7), Beta (B.1.351), Gamma (P.1), Delta (B.1.617.2), and Omicron (BA.1) variants of concern (Figure 2, Figure S3). We observed successful detection of 0.05 ng/mL for the Alpha, Gamma,

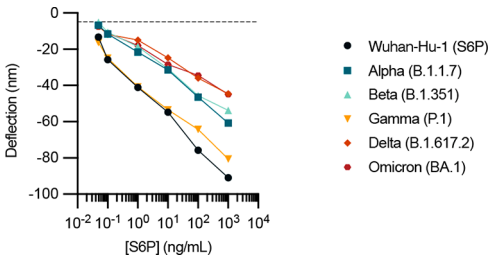

Figure 2. Detection of purified S trimer representing current and historical SARS-CoV-2 variants of concern. Cantilever deflection after 15 min of equilibration (mean ± SEM, n = 3). The dashed horizontal line indicates the deflection LOD cutoff (average of the combined negative control measurements ± 3 standard deviations), and an absence of error bars indicates error within the marker.

https://doi.org/10.1021/acs.analchem.2c01221
Anal. Chem. 2022, 94, 8105−8109

Delta, and Omicron S trimer and 0.1 ng/mL of the Beta S trimer, with the deflection crossing the limit of detection cutoff around 5 min at the lowest detectable concentration (Figure S3a−e). We observed varying levels of deflection for the different S trimer variants (Figure 2), possibly due to heterogeneity in the different preparations of recombinant S trimer. These measurements demonstrate the ability of TRI2-2 functionalized cantilevers to detect antigens from different SARS-CoV-2 variants of concern.

Given the highly sensitive detection of purified S trimer, we next sought to determine if TRI2-2 functionalized cantilevers could be utilized to detect SARS-CoV-2 in patient samples. Residual diagnostic nasopharyngeal swabs were collected from patients presenting to Northwestern Memorial Hospital between March of 2021 and January of 2022. Cycle threshold (Ct) values were calculated by quantitative reverse transcription and PCR (RT-qPCR) as a proxy for SARS-CoV-2 viral load. The genotype of the virus in each sample was determined by whole-genome sequencing using the ARTIC protocol. Pango lineages were assigned to the consensus sequences using pangolin software to assign variant designations. Specimens that tested negative for SARS-CoV-2 or positive for another respiratory virus (influenza A virus) were used as negative controls.

We tested 27 RT-qPCR positive and 5 RT-qPCR negative patient samples (Table S1), including samples from early in 2021, samples from confirmed Alpha (B.1.1.7) variant infections, and samples from confirmed Omicron (BA.1) variant infections (Figure 3a, Figure S4a−c). A linear

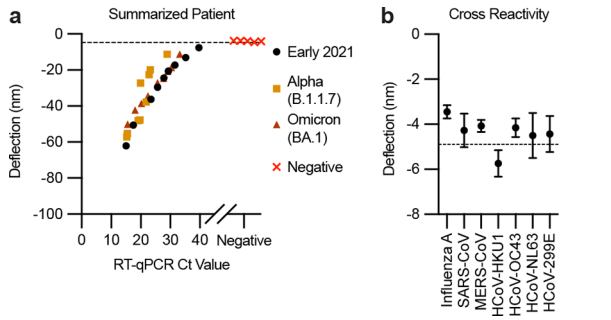

Figure 3. Measurement of SARS-CoV-2 in nasopharyngeal swabs from infected individuals and of cross reactivity with other related viruses. (a) Comparison of the RT-qPCR Ct value and cantilever deflection after 15 min for the tested patient samples (mean ± SEM, n = 3). (b) Deflection of cantilevers after 15 min in response to recombinant purified SARS-CoV, MERS-CoV, HCoV-HKU1, HCoV-OC43, HCoV-NL63, and HCoV-299E spike protein (1 000 ng/mL) and against a patient nasopharyngeal swab RT-qPCR positive for influenza A (Ct = 19.33) (mean ± SEM, n = 3). For all plots, the dashed horizontal line indicates the deflection LOD cutoff (average of the combined negative control measurements ± 3 standard deviations) and an absence of error bars indicates error within the marker.

relationship was observed between the Ct value measured by RT-qPCR and cantilever deflection (Figure 3a) and thus a log−linear relationship with viral RNA copy number (Table S2). Consistent with the results using purified antigen, patient samples exhibited detection after approximately 5 min of incubation of the sample with the sensor. For the lowest Ct value sample tested (Ct = 39), we observed signal significantly different from all negative patient samples (Figure S4a) at 7 min (p < 0.05, 2-way ANOVA with Sidak's multiple comparisons test), indicating confident detection of antigen concentration corresponding to 96 viral RNA copies per mL (Table S2). SARS-CoV-2 RT-qPCR negative samples from five patients exhibited little deflection (Figure 3a), comparable to the buffer negative control (Figure 1d). To probe the cross reactivity of our sensor, we tested an RT-qPCR positive influenza A sample and recombinant purified spike proteins from other human coronaviruses and observed little deflection at a concentration of 1 000 ng/mL (Figure 3b, Figure S4e), with only HCoV-HKU1 exhibiting limited signal above the average background deflection (within 6 standard deviations). These results indicate our sensor does not have significant cross-reactivity for these tested viruses.

Here, we have used a multivalent minibinder functionalized nanomechanical sensor to detect the S trimer antigen from different SARS-CoV-2 variants of concern. Our sensor can detect femtomolar concentrations of antigen and our data for patient samples suggest an LOD that is comparable to nucleic acid tests with amplification[26] and >2 orders of magnitude better than currently authorized rapid antigen tests.[5,8,10] The sensor does not require amplification and shows results in patient samples in 5 min. Taken together, these benefits indicate that the developed sensor has promise as a clinical diagnostic, although more samples must be evaluated to determine clinical sensitivity and specificity.[28] Using an alternative detection modality like a metal-oxide semiconductor field-effect transistor (MOSFET) detector for electronic readout in a hand-held device could make it accessible in point-of-care settings.[17] Computationally designed binding proteins and nanomechanical sensors will enable fast and sensitive detection of biomarkers for disease diagnosis for SARS-CoV-2 and other diseases.

■ ASSOCIATED CONTENT

Supporting Information

The Supporting Information is available free of charge at https://pubs.acs.org/doi/10.1021/acs.analchem.2c01221.

Chemical reagents and materials; recombinant protein expression and purification; cantilever surface biofunctionalization; optical detection method; patient sample collection and Ct value calculation; Ct value calculation and variant identification; Figure S1, SEM micrograph of a microcantilever device; Figure S2, histogram of measured error for all cantilever deflection measurements; Figure S3, kinetic detection of purified S trimer representing current and historical SARS-CoV-2 variants of concern; Figure S4, measurement of SARS-CoV-2 in nasopharyngeal swabs from infected individuals and of cross reactivity with other related viruses; Table S1, summary of the measured RT-qPCR Ct values, lineage designations, and GISAID identifiers for all reported patient samples (as available); and Table S2, summary of the measured RT-qPCR Ct values, their corresponding concentration of RNA (copies/mL), and their measured deflection (± standard deviation) for all reported patient samples (PDF)

Supporting raw data (XLSX)

■ AUTHOR INFORMATION

Corresponding Authors

Michael C. Jewett − *Department of Chemical and Biological Engineering and Center for Synthetic Biology and Chemistry*

https://doi.org/10.1021/acs.analchem.2c01221
Anal. Chem. 2022, 94, 8105−8109

of Life Processes Institute, Northwestern University, Evanston, Illinois 60208, United States; Robert H. Lurie Comprehensive Cancer Center, Northwestern University, Chicago, Illinois 60611, United States; orcid.org/0000-0003-2948-6211; Email: m-jewett@northwestern.edu

Vinayak P. Dravid − *Department of Material Science and Engineering and NUANCE Center and Chemistry of Life Processes Institute, Northwestern University, Evanston, Illinois 60208, United States; Robert H. Lurie Comprehensive Cancer Center, Northwestern University, Chicago, Illinois 60611, United States;* orcid.org/0000-0002-6007-3063; Email: v-dravid@northwestern.edu

Authors

Dilip Kumar Agarwal − *Department of Material Science and Engineering and NUANCE Center, Northwestern University, Evanston, Illinois 60208, United States;* orcid.org/0000-0002-7330-1491

Andrew C. Hunt − *Department of Chemical and Biological Engineering and Center for Synthetic Biology, Northwestern University, Evanston, Illinois 60208, United States;* orcid.org/0000-0001-9620-593X

Gajendra S. Shekhawat − *Department of Material Science and Engineering and NUANCE Center, Northwestern University, Evanston, Illinois 60208, United States;* orcid.org/0000-0003-3497-288X

Lauren Carter − *Department of Biochemistry and Institute for Protein Design, University of Washington, Seattle, Washington 98195, United States*

Sidney Chan − *Department of Biochemistry and Institute for Protein Design, University of Washington, Seattle, Washington 98195, United States*

Kejia Wu − *Department of Biochemistry and Institute for Protein Design, University of Washington, Seattle, Washington 98195, United States*

Longxing Cao − *Department of Biochemistry and Institute for Protein Design, University of Washington, Seattle, Washington 98195, United States*

David Baker − *Department of Biochemistry, Institute for Protein Design, and Howard Hughes Medical Institute, University of Washington, Seattle, Washington 98195, United States*

Ramon Lorenzo-Redondo − *Department of Medicine, Division of Infectious Diseases and Center for Pathogen Genomics and Microbial Evolution, Robert J. Havey Institute for Global Health, Northwestern University Feinberg School of Medicine, Chicago, Illinois 60611, United States*

Egon A. Ozer − *Department of Medicine, Division of Infectious Diseases and Center for Pathogen Genomics and Microbial Evolution, Robert J. Havey Institute for Global Health, Northwestern University Feinberg School of Medicine, Chicago, Illinois 60611, United States;* orcid.org/0000-0002-7131-3691

Lacy M. Simons − *Department of Medicine, Division of Infectious Diseases and Center for Pathogen Genomics and Microbial Evolution, Robert J. Havey Institute for Global Health, Northwestern University Feinberg School of Medicine, Chicago, Illinois 60611, United States*

Judd F. Hultquist − *Department of Medicine, Division of Infectious Diseases and Center for Pathogen Genomics and Microbial Evolution, Robert J. Havey Institute for Global Health, Northwestern University Feinberg School of Medicine, Chicago, Illinois 60611, United States*

Complete contact information is available at: https://pubs.acs.org/10.1021/acs.analchem.2c01221

Author Contributions

[×]D.K.A. and A.C.H. contributed equally. D.K.A. performed the cantilever experiments. A.C.H. expressed and purified the minibinders. D.K.A. and A.C.H. designed the experiments, analyzed the data, and wrote the initial manuscript. L.C. provided purified S trimer for the Alpha, Beta, and Gamma variants. K.W. and L.C. designed the minibinders used in this manuscript. G.S.S., D.B., M.C.J., J.F.H. and V.P.D. supervised the research. J.F.H., E.A.O., R.L.-R., and L.M.S. collected the patient specimens, calculated the viral load, and performed variant identification. All authors edited the manuscript and have given approval for the final version.

Notes

The authors declare the following competing financial interest(s): A.C.H., M.C.J., L.C., K.W., and D.B. are co-inventors on provisional patent applications covering the minibinders described in this manuscript (Application No. PCT/US2021/034069, Title: SARS-COV-2 inhibitors). M.C.J. is a cofounder of SwiftScale Biologics, Stemloop, Inc., Design Pharmaceuticals, and Pearl Bio. The interests of M.C.J. are reviewed and managed by Northwestern University in accordance with their conflict of interest policies. All other authors declare no competing interests.

■ ACKNOWLEDGMENTS

This work made use of the SPID facilities of the NU*ANCE* Center at Northwestern University which has received support from Soft and Hybrid Nanotechnology Experimental (SH_yNE) Resource (Grant NSF-ECCS-1542205), MRSEC Program (Grant NSF DMR-1121262) at the Materials Research Center; the International Institute for Nanotechnology (IIN); the Keck Foundation; and the State of Illinois, through the IIN. This work was supported by grant from the National Heart, Lung and Blood Institute Award Number 1400-SUB/3U54HL119810-07S1: Rapid Diagnostics of SARS-C0 V-2 of Asymptomatic people returning to work and school. A.C.H. was funded by a National Defense Science and Engineering Graduate (NDSEG) Fellowship Program (Grant NDSEG-36373). M.C.J. gratefully acknowledges the Packard Foundation, the Defense Threat Reduction Agency Grants HDTRA-12-01-0004 and HDTRA-12-11-0038, and the National Science Foundation Rapid Grant MCB-2028651. This research was supported in part through the computational resources and staff contributions provided for the Quest High Performance Computing Facility at Northwestern University, which is jointly supported by the Office of the Provost, the Office for Research, and Northwestern University Information Technology. Funding for patient sample collection and variant identification was provided by a Dixon Translational Research Grant made possible by the generous support of the Dixon Family Foundation (E.A.O. and J.F.H.); a COVID-19 Supplemental Research award from the Northwestern Center for Advanced Technologies (NUCATS, J.F.H.); a CTSA supplement to NCATS UL1 TR002389 (J.F.H., E.A.O., R.L.-R.); a supplement to the Northwestern University Cancer Center P30 CA060553 (J.F.H.); the NIH-supported Third Coast CFAR P30 AI117943 (R.L.-R., J.F.H.); NIH Grant R21 AI163912 (J.F.H.); NIH Grant U19 AI135964 (E.A.O.); and through a generous contribution from the Walder Foundation

Foundation's Chicago Coronavirus Assessment Network (Chicago CAN) Initiative (J.F.H., E.A.O., R.L.-R.).

REFERENCES

(1) Vandenberg, O.; Martiny, D.; Rochas, O.; van Belkum, A.; Kozlakidis, Z. *Nat. Rev. Microbiol.* **2021**, *19* (3), 171−183.
(2) Benda, A.; Zerajic, L.; Ankita, A.; Cleary, E.; Park, Y.; Pandey, S. *Sensors (Basel)* **2021**, *21* (19), 6581.
(3) Pavelka, M.; Van-Zandvoort, K.; Abbott, S.; Sherratt, K.; Majdan, M.; Jarcuska, P.; Krajci, M.; Flasche, S.; Funk, S. *Science* **2021**, *372*, 635−641.
(4) Mina, M. J.; Peto, T. E.; García-Fiñana, M.; Semple, M. G.; Buchan, I. E. *Lancet* **2021**, *397* (10283), 1425−1427.
(5) Corman, V. M.; Haage, V. C.; Bleicker, T.; Schmidt, M. L.; Mühlemann, B.; Zuchowski, M.; Jo, W. K.; Tscheak, P.; Möncke-Buchner, E.; Müller, M. A.; Krumbholz, A.; Drexler, J. F.; Drosten, C. *Lancet Microbe* **2021**, *2* (7), e311−e319.
(6) Lanser, L.; Bellmann-Weiler, R.; Öttl, K.-W.; Huber, L.; Griesmacher, A.; Theurl, I.; Weiss, G. *Infection* **2021**, *49* (3), 555−557.
(7) Wölfel, R.; Corman, V. M.; Guggemos, W.; Seilmaier, M.; Zange, S.; Müller, M. A.; Niemeyer, D.; Jones, T. C.; Vollmar, P.; Rothe, C.; Hoelscher, M.; Bleicker, T.; Brünink, S.; Schneider, J.; Ehmann, R.; Zwirglmaier, K.; Drosten, C.; Wendtner, C. *Nature* **2020**, *581* (7809), 465−469.
(8) Perchetti, G. A.; Huang, M.-L.; Mills, M. G.; Jerome, K. R.; Greninger, A. L. *J. Clin. Microbiol.* **2021**, *59* (3), e02880-20.
(9) Adamson, B.; Sikka, R.; Wyllie, A. L.; Premsrirut, P. *medRxiv* **2022**, 2022.01.04.22268770.
(10) Frediani, J. K.; Levy, J. M.; Rao, A.; Bassit, L.; Figueroa, J.; Vos, M. B.; Wood, A.; Jerris, R.; Van Leung-Pineda; Gonzalez, M. D.; Rogers, B. B.; Mavigner, M.; Schinazi, R. F.; Schoof, N.; Waggoner, J. J.; Kempker, R. R.; Rebolledo, P. A.; O'Neal, J. W.; Stone, C.; Chahroudi, A.; Morris, C. R.; Suessmith, A.; Sullivan, J.; Farmer, S.; Foster, A.; Roback, J. D.; Ramachandra, T.; Washington, C.; Le, K.; Cordero, M. C.; Esper, A.; Nehl, E. J.; Wang, Y. F.; Tyburski, E. A.; Martin, G. S.; Lam, W. A. *Sci. Rep.* **2021**, *11*, 14604.
(11) Osterman, A.; Badell, I.; Basara, E.; Stern, M.; Kriesel, F.; Eletreby, M.; Öztan, G. N.; Huber, M.; Autenrieth, H.; Knabe, R.; Späth, P. M.; Muenchhoff, M.; Graf, A.; Krebs, S.; Blum, H.; Durner, J.; Czibere, L.; Dächert, C.; Kaderali, L.; Baldauf, H.-M.; Keppler, O. T. *Med. Microbiol. Immunol.* **2022**, *211*, 105.
(12) Agarwal, D. K.; Nandwana, V.; Henrich, S. E.; Josyula, V. P. V. N.; Thaxton, C. S.; Qi, C.; Simons, L. M.; Hultquist, J. F.; Ozer, E. A.; Shekhawat, G. S.; Dravid, V. P. *Biosens. Bioelectron.* **2022**, *195*, 113647.
(13) Agarwal, D. K.; Prasad, A.; Vinchurkar, M.; Gandhi, S.; Prabhakar, D.; Mukherji, S.; Rao, V. R. *Appl. Nanosci.* **2018**, *8* (5), 1031−1042.
(14) Lavrik, N. V.; Sepaniak, M. J.; Datskos, P. G. *Rev. Sci. Instrum.* **2004**, *75* (7), 2229−2253.
(15) Agarwal, D. K.; Kushagra, A.; Ashwin, M.; Shukla, A. S.; Palaparthy, V. *Nanotechnology* **2020**, *31* (11), 115503.
(16) Tamayo, J.; Kosaka, P. M.; Ruz, J. J.; San Paulo, Á.; Calleja, M. *Chem. Soc. Rev.* **2013**, *42* (3), 1287−1311.
(17) Shekhawat, G.; Tark, S.-H.; Dravid, V. P. *Science* **2006**, *311* (5767), 1592−1595.
(18) Starr, T. N.; Greaney, A. J.; Addetia, A.; Hannon, W. W.; Choudhary, M. C.; Dingens, A. S.; Li, J. Z.; Bloom, J. D. *Science* **2021**, *371* (6531), 850−854.
(19) Cao, L.; Goreshnik, I.; Coventry, B.; Case, J. B.; Miller, L.; Kozodoy, L.; Chen, R. E.; Carter, L.; Walls, A. C.; Park, Y.-J.; Strauch, E.-M.; Stewart, L.; Diamond, M. S.; Veesler, D.; Baker, D. *Science* **2020**, *370* (6515), 426−431.
(20) Hunt, A. C.; Case, J. B.; Park, Y.-J.; Cao, L.; Wu, K.; Walls, A. C.; Liu, Z.; Bowen, J. E.; Yeh, H.-W.; Saini, S.; Helms, L.; Zhao, Y. T.; Hsiang, T.-Y.; Starr, T. N.; Goreshnik, I.; Kozodoy, L.; Carter, L.; Ravichandran, R.; Green, L. B.; Matochko, W. L.; Thomson, C. A.; Vögeli, B.; Krüger, A.; VanBlargan, L. A.; Chen, R. E.; Ying, B.; Bailey, A. L.; Kafai, N. M.; Boyken, S. E.; Ljubetič, A.; Edman, N.; Ueda, G.; Chow, C. M.; Johnson, M.; Addetia, A.; Navarro, M. J.; Panpradist, N.; Gale, M., Jr; Freedman, B. S.; Bloom, J. D.; Ruohola-Baker, H.; Whelan, S. P. J.; Stewart, L.; Diamond, M. S.; Veesler, D.; Jewett, M. C.; Baker, D. *Sci. Transl. Med.* **2022**, eabn1252.
(21) Holstein, C. A.; Chevalier, A.; Bennett, S.; Anderson, C. E.; Keniston, K.; Olsen, C.; Li, B.; Bales, B.; Moore, D. R.; Fu, E.; Baker, D.; Yager, P. *Anal. Bioanal. Chem.* **2016**, *408* (5), 1335−1346.
(22) Anderson, C. E.; Holstein, C. A.; Strauch, E.-M.; Bennett, S.; Chevalier, A.; Nelson, J.; Fu, E.; Baker, D.; Yager, P. *Anal. Chem.* **2017**, *89* (12), 6608−6615.
(23) Silverman, A. D.; Karim, A. S.; Jewett, M. C. *Nat. Rev. Genet.* **2020**, *21* (3), 151−170.
(24) Jewett, M. C.; Calhoun, K. A.; Voloshin, A.; Wuu, J. J.; Swartz, J. R. *Mol. Syst. Biol.* **2008**, *4*, 220.
(25) Jewett, M. C.; Swartz, J. R. *Biotechnol. Bioeng.* **2004**, *86* (1), 19−26.
(26) Fung, B.; Gopez, A.; Servellita, V.; Arevalo, S.; Ho, C.; Deucher, A.; Thornborrow, E.; Chiu, C.; Miller, S. *J. Clin. Microbiol.* **2020**, *58* (9), e01535-20.
(27) Hsieh, C.-L.; Goldsmith, J. A.; Schaub, J. M.; DiVenere, A. M.; Kuo, H.-C.; Javanmardi, K.; Le, K. C.; Wrapp, D.; Lee, A. G.; Liu, Y.; Chou, C.-W.; Byrne, P. O.; Hjorth, C. K.; Johnson, N. V.; Ludes-Meyers, J.; Nguyen, A. W.; Park, J.; Wang, N.; Amengor, D.; Lavinder, J. J.; Ippolito, G. C.; Maynard, J. A.; Finkelstein, I. J.; McLellan, J. S. *Science* **2020**, *369* (6510), 1501−1505.
(28) Bujang, M. A.; Adnan, T. H. *J. Clin. Diagn. Res.* **2016**, *10* (10), YE01−YE06.

https://doi.org/10.1021/acs.analchem.2c01221
Anal. Chem. 2022, 94, 8105−8109